JCTC Journal of Chemical Theory and Computation

Article

pubs.acs.org/JCTC

Excited-State Proton Transfer Controls Irreversibility of Photoisomerization in Mononuclear Ruthenium(II) Monoaquo Complexes: A DFT Study

Lina Ding,[†,‡] Lung Wa Chung,[†] and Keiji Morokuma*[,†]

[†]Fukui Institute for Fundamental Chemistry, Kyoto University, 34-4 Takano Nishihiraki-cho, Kyoto 606-8103, Japan

[‡]School of Pharmaceutical Sciences, Zhengzhou University, 100 Kexue Avenue, Zhengzhou, Henan 450001, China

Supporting Information

ABSTRACT: The detailed DFT investigation clears the working mechanism of the irreversible photoisomerization of *trans*-[Ru(tpy)(pynp)(OH_2)]$^{2+}$ (TA) and *cis*-[Ru(tpy)(pynp)(OH_2)]$^{2+}$ (CA) complexes. Both TA and CA complexes present two types of low lying triplet states, one resulting from a triplet metal−ligand charge-transfer (T_{MLCT}) and the other from a triplet metal-centered d−d transition (T_{MC}). The vertical excitation of the singlet ground state of the complexes leads to a singlet excited state, which undergoes ultrafast decay to the corresponding T_{MLCT}. For TA, this T_{MLCT} transforms with a low barrier to a T_{MC} state. The dissociative nature of the T_{MC} state leads to easy water removal to produce a five-coordinate intermediate that can isomerize via rotation of a pynp ligand and proceed towards the CA product. For CA, however, during this excitation and intersystem crossing process, an excited-state proton transfer (ESPT) occurs and the resultant T_{MLCT} is very much stabilized with a very strong Ru(II)−OH bond; the high barrier from this T_{MLCT} blocks conversion to a T_{MC} state and thus prevents isomerization from the *cis* to the *trans* isomer. This high barrier also prevents the possibility of the isomerization process from TA to CA solely on the adiabatic triplet pathway. Instead, crossing points ($X_{MC\text{-}CB}$, $X_{MC\text{-}CA}$) near the minimum of the triplet metal-centered state of the *cis* isomer provide nonadiabatic decay channels to the ground-state $S_{0\text{-}CA}$, which completes the photoisomerization pathway from TA to CA.

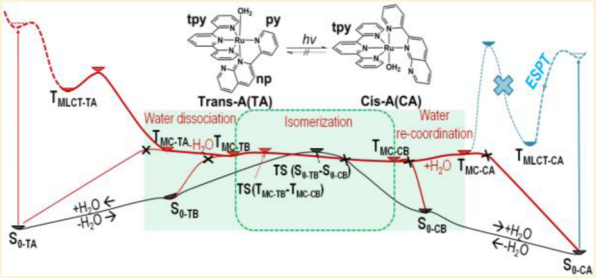

INTRODUCTION

Photoinduced or phototriggered isomerization can utilize photonic energy for selective bond-breaking and bond-making reactions. These types of reactions between two or more optically and electronically distinct isomers or metastable species have been observed in a broad variety of molecules, including stilbene and its derivatives,[1] rhodopsins,[2] and fluorescence proteins,[3] as well as transition metal complexes including photochromic ruthenium(II) polypyridine sulfoxide and polypyridyl mononuclear ruthenium(II) aquo (PMRA) and other ruthenium(II) complexes.[4−6] Except for ruthenium polypyridine sulfoxide complexes, mechanistic studies on PMRA[5] are scarce. The importance of photoisomerization in PMRA lies in the fact that the two isomers have different potential catalytic abilities for water oxidation into molecular oxygen,[7] one of the key reactions involved in solar energy conversion.

Recently, an irreversible photo-isomerization[5c,d] of *trans*-[Ru(tpy)(pynp)(OH_2)]$^{2+}$ (TA) to *cis*-[Ru(tpy)(pynp)-(OH_2)]$^{2+}$ (CA) complex (tpy = 2,2′:6′,2″-terpyridine; pynp = 2-(2-pyridyl)-1,8-naphthyridine, Scheme 1) has been observed and characterized by experimental techniques, such as X-ray crystallographic analysis, NMR spectroscopy, and cyclic voltammetry. Importantly, the redox and water oxidation reactions were reported to be significantly controlled by the photoisomerization. Yagi proposed a mechanism for the photoisomerization: visible-light irradiation of TA can generate a state resulting from a metal−ligand charge-transfer, which is followed by a state resulting from a metal-centered d−d transition, on which an aquo ligand could dissociate to form a five-coordinate [Ru(tpy)(pynp)]$^{2+}$ intermediate, and then a

Scheme 1. Photoisomerization of *trans*-[Ru(tpy)(pynp)(OH_2)]$^{2+}$ (TA) to *cis*-[Ru(tpy)(pynp)(OH_2)]$^{2+}$ (CA), with Atom and Group Labels

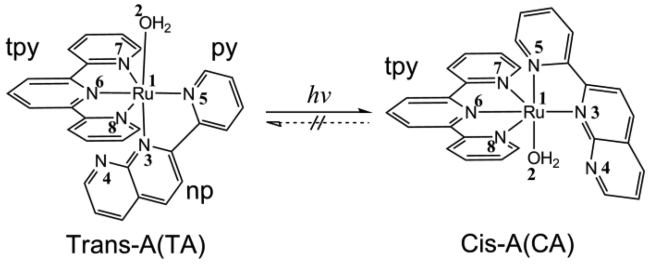

Received: November 13, 2013
Published: January 16, 2014

Table 1. Selected Ru-Centered Bond Distances (atom numbers defined in Scheme 1; in Å) for the Ground-State TA and CA at the M06/BS1 Level in Water, as Well as X-ray Structures

structure	Ru1−O2	Ru1−N3	Ru1−N5	Ru1−N6	Ru1−N7	Ru1−N8	O2−N4
X-ray (TA)	2.199(7)	2.059(8)	2.062(9)	1.975(9)	2.087(8)	2.075(8)	-
$S_{0\text{-}TA}$	2.219	2.088	2.099	1.996	2.106	2.106	-
X-ray (CA)	2.121(3)	2.109(3)	2.027(4)	1.970(4)	2.080(4)	2.070(4)	2.659
$S_{0\text{-}CA}$	2.200	2.134	2.045	1.992	2.110	2.101	2.702

water molecule recoordinates to the metal center of the intermediate from the opposite side of the tpy plane to form the CA isomer. The proposed Ru−O bond cleavage involved in the water dissociation was implicated by the observed activation energy of the photoisomerization (41.7 kJ mol^{-1}),[5c] which is similar to that for the water exchange in ruthenium aquo complexes (50.6−87.8 kJ mol^{-1}).[8] However, it is still a puzzle why the isomerization is irreversible.

In spite of the challenges associated with the characterization of the excited state properties and mechanisms of transition metal complexes (due to the presence of different electronic states in a narrow energy range as well as to their fast intersystem crossing kinetics,[9] theoretical studies have successfully been conducted, including the study of photophysical properties[10] and isomerization mechanisms[5b,e,11] at different levels of theory (such as TDDFT//DFT, RASPT2//RASSCF). Salassa et al.[11a] reported a DFT study on the photodissociation mechanism and singlet/triplet excited-state properties of $[Ru(bpy)_2L_2]^{2+}$ (L = neuroactive aromatic or aliphatic amine) complexes and pointed out that electrons in two antibonding orbitals (d_{z2} and $d_{x2}-d_{y2}$) in the metal-centered state are responsible for the ligand release. Göttle et al.[11b] suggested that an efficient nonadiabatic photoisomerization pathway via minimum energy crossing points in photochromic ruthenium sulfoxide complexes ($[Ru(bpy)_2(OSO)]^+$) is favorable and highlighted for the first time the central role of triplet metal-centered states. Planas et al.[5b] employed a density functional theory and time-dependent density functional theory (using the M06 family) to study photoisomerization from *cis*-$[Ru^{II}(bpy)_2(H_2O)_2]^{2+}$ to *trans*-$[Ru^{II}(bpy)_2(H_2O)_2]^{2+}$ via water dissociation, intersystem crossing, and water recoordination. These previous studies provided important insights into the photochemical reactions of transition metal complexes. The *irreversible* isomerization process in PMRA is quite different from these well-studied systems. Understanding the working mechanism of the irreversibility of isomerization is essential and should be critical for expanding potential applications.

In this study, we explored the photoinduced nonadiabatic isomerization paths between *trans*-$[Ru(tpy)(pynp)(H_2O)]^{2+}$ (TA) and *cis*-$[Ru(tpy)(pynp)(H_2O)]^{2+}$ (CA) on the lowest triplet and singlet states by density functional theory (DFT) calculations. Several minimum energy crossing points (MSX) were located and characterized to connect the two adiabatic potential energy surfaces (PESs) for nonadiabatic pathways. Interestingly, excited-state proton transfer (ESPT) occurred only in the minimum of $T_{MLCT\text{-}CA}$ with a stronger Ru(II)−OH bond suppressing the transition to $T_{MC\text{-}CA}$ and, thus, the adiabatic triplet pathway from CA to TA. The findings of the present study should shed light on the working mechanism of the irreversible isomerization processes of PMRA.

COMPUTATIONAL DETAILS

DFT was employed to optimize the ground-state and the first triplet-state structures, while time-dependent (TD) DFT theory was used to analyze the nature of excitation states at the ground-state optimized geometries (i.e., Franck−Condon point). We used M06[12] functional in all the calculations, since M06 was shown to provide a better description of charge-transfer excitation[13] as well as potential energy surfaces.[14] The LanL2DZ[15] basis set and effective core potential were used for the Ru atom, while the split-valence 6-31G(d,p) basis set[16] was applied for the other atoms (C, N, O, and H). This set is called BS1. Frequency calculations at the M06/BS1 level of theory were carried out to confirm stationary points as minima (no imaginary frequency) or transition states (one imaginary frequency). The zero-point energies and the thermal correction data were obtained at 298.15 K and 1 atm within the harmonic approximation at the optimized structures. Intrinsic reaction coordinates (IRCs) were calculated to verify the connection of the transition states to their relevant reactants and products. Mulliken spin density on the ruthenium atom and visual inspection of molecular orbitals were used to characterize and distinguish the metal−ligand charge transfer (MLCT) and metal-centered (MC) characters of excited states. All calculations above were performed by the Gaussian09[17] package.

In order to find nonadiabatic pathways for photoisomerization, we searched for minimum energy crossing points (MSXs). These crossing points were optimized at M06/BS1 level using an MSX optimizer implemented in the GRRM11 program.[18,19] To consider whether the effect of the basis set is negligible, a larger basis set BS2 (SDD for Ru and 6-311G(d,p) for the rest, termed as BS2) has been used to refine the energetics of the optimized MSXs and stationary points as well as transition states. As shown in Supporting Information Table S1, the relative energies are changed only by ∼1.5−3 kcal/mol compared with the BS1 and mechanistic picture is not changed. The conductor-like polarizable continuum model method (CPCM)[20] was chosen to consider the solvent effect of the water environment. On the basis of the optimized geometries with the CPCM model, bulk solvent effects were also considered implicitly by performing single-point energy calculations with the SMD polarizable continuum model[21] as implemented in Gaussian 09, which did not change the mechanistic picture. Therefore, considering the consistency, we mainly discuss the results with BS1 with CPCM model throughout the paper.

For reactions in which the number of molecules changes, the entropic contribution is important. Therefore, in the present paper, we use the Gibbs free energy with full contribution of the entropic effect for discussion, except for the crossing points (nonstationary points) where the electronic energy (without vibrational or entropic contribution) was used. Fortunately, qualitative discussions and conclusions based on the Gibbs free energy are essentially the same as those from the electronic energy only.

dx.doi.org/10.1021/ct400982r | J. Chem. Theory Comput. 2014, 10, 668−675

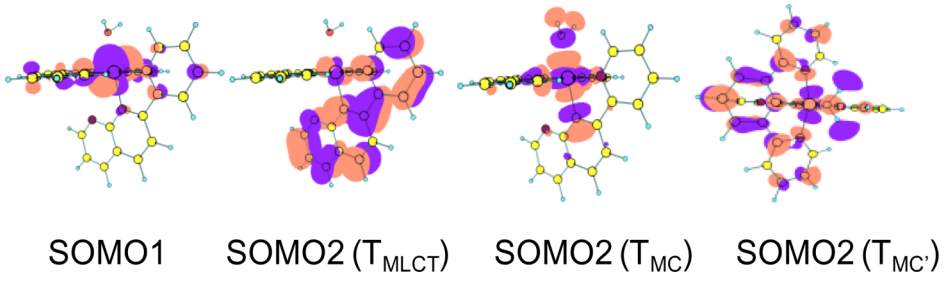

Figure 1. SOMOs for the $T_{MLCT\text{-}TA}$, $T_{MC\text{-}TA}$, and $T_{MC'\text{-}TA}$ states at $S_{0\text{-}TA}$.

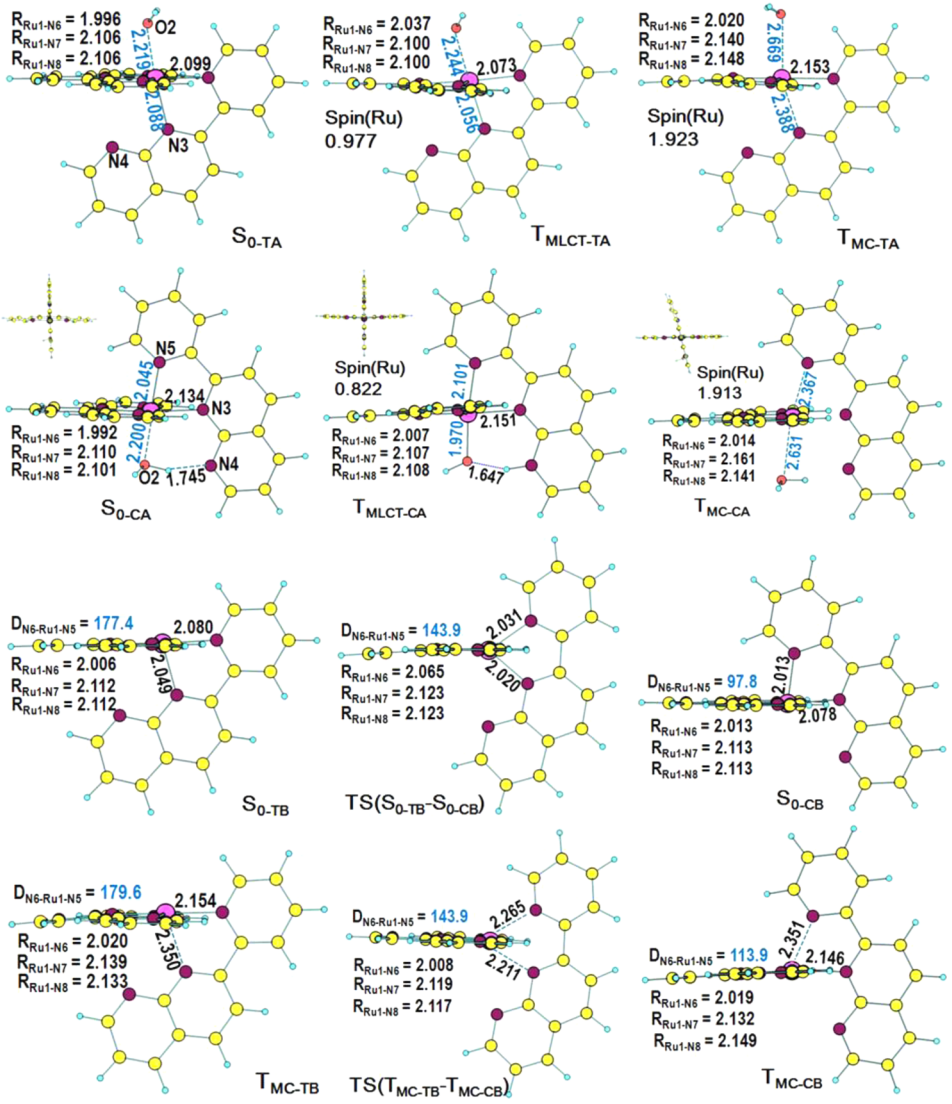

Figure 2. Key parameters of stationary points and transition states (distances, Å; angles, deg) at the M06/BS1 level in water.

■ RESULTS AND DISCUSSIONS

A. Minimum Structures of the Singlet and Triplet States. The ground-state (singlet) minima of complexes TA and CA, named as $S_{0\text{-}TA}$ and $S_{0\text{-}CA}$, respectively, were obtained. As shown in Table 1, the selected Ru-centered geometrical parameters for both $S_{0\text{-}TA}$ and $S_{0\text{-}CA}$ are similar to their corresponding X-ray structures.[5c] Here, the largest difference comes from the overestimation of these interactions as was seen previously for different groups with hybrid functional calculations.[22] Two structures, $S_{0\text{-}TA}$ and $S_{0\text{-}CA}$, display similar frontier orbitals and orbital energies (Supporting Information Table S2). However, due to the existence of one hydrogen-bond (O2—H···N4) in $S_{0\text{-}CA}$ and presumably some repulsive interaction between the N4 lone pair and π orbital of the tpy ring in $S_{0\text{-}TA}$, $S_{0\text{-}CA}$ is more stable than $S_{0\text{-}TA}$ by 7.7 (8.6) kcal/mol in the Gibbs free energy (the electronic energy in parentheses).

For both $S_{0\text{-}TA}$ and $S_{0\text{-}CA}$, a vertical excitation with the largest oscillator strength (f) value by the TD-M06 method belongs to a singlet metal-to-ligand charge-transfer state (S_{MLCT}). This absorption peak is calculated to be 2.55 eV (487 nm) for $S_{0\text{-}TA}$

dx.doi.org/10.1021/ct400982r | J. Chem. Theory Comput. 2014, 10, 668−675

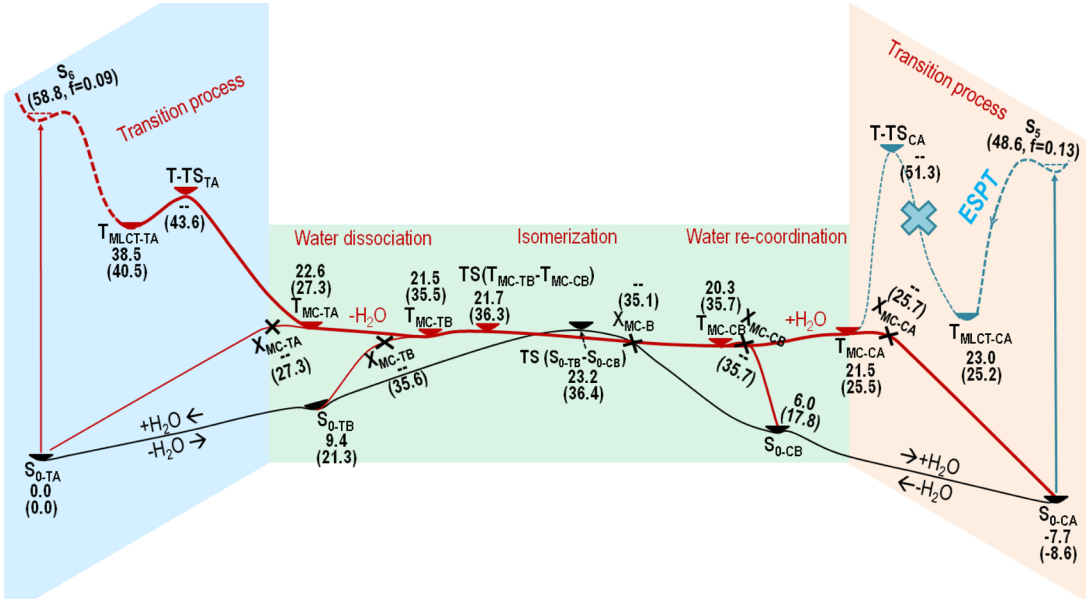

Figure 3. Profiles of Gibbs and electronic energies (in parentheses) (in kcal/mol) between *trans*-A (TA) and *cis*-A (CA) along the adiabatic and nonadiabatic photoisomerization pathways on the ground singlet state (black curve) and lowest triplet state (red and blue lines) in water.

and 2.48 eV (501 nm) for $S_{0\text{-}CA}$ (without ZPE), which is slightly overestimated from the experimental peaks (527 and 524 nm, respectively). In addition, a singlet metal-centered excited state (S_{MC}), which plays a crucial role in photodissociation pathway (see discussion below), is found to be higher in energy than S_{MLCT}, with a vertical excitation energy of 2.78−2.84 eV for TA and 3.13 eV for CA.

There are two triplet states resulting from two excitations from the S_0 ground state. One results from a MLCT that will be referred to as T_{MLCT}, while the other results from an MC that will be referred to as T_{MC}. Correspondingly, two different types of triplet-state minimum structures were located for each of the CA and TA isomers and named as triplet metal−ligand charge-transfer structure ($T_{MLCT\text{-}CA}$ and $T_{MLCT\text{-}TA}$) and triplet metal-centered structures ($T_{MC\text{-}CA}$ and $T_{MC\text{-}TA}$; $T_{MC'\text{-}CA}$ and $T_{MC'\text{-}TA}$), which represent the d(Ru) → π^*(ligand) and d(Ru) → d(Ru) excitations, respectively. The MO analysis (Figure 1, Supporting Information Tables S3 and S4) shows that SOMO1 of all T_{MLCT}, T_{MC}, and $T_{MC'}$ structures is mainly a Ru-centered d orbital. SOMO2 of T_{MLCT} is mainly delocalized on the pynp ligand, while that of T_{MC} has a Ru-ligand σ^* character along the axis between Ru and water as well as the ligand *trans* to water and that of $T_{MC'}$ has a Ru-ligand σ^* character along the N7−Ru−N8 axis of the tpy ligand.

The structure of $T_{MLCT\text{-}CA}$ deserves special attention (Figure 2 and Supporting Information Figure S1). Here the excited-state proton-transfer (ESPT) from the water ligand to the N4 atom of pynp has taken place spontaneously keeping the O2−N4 distance almost unchanged. This is because, in the MLCT state, the pynp ligand becomes much more negatively charged and strongly attracts a proton from the metal-coordinating water molecule in CA configuration. The interaction between the Ru and OH^- becomes stronger (1.970 Å). On the other hand, in $T_{MLCT\text{-}TA}$, the negatively charged pynp ligand is far away from the coordinated water molecule and ESPT from this water to pynp cannot take place.[23] The Gibbs (electronic) energy of $T_{MLCT\text{-}CA}$ is 23.0 (25.2) kcal/mol, relative to that for the ground state $S_{0\text{-}TA}$, and is lower in energy than that of $T_{MLCT\text{-}TA}$ by 15.5 (15.3) kcal/mol. The dipole moment of $T_{MLCT\text{-}TA}$ is found to increase by 6.3 D, while that of $T_{MLCT\text{-}CA}$ increased only by 3.9 D, relative to that of $S_{0\text{-}TA}$, at the M06/BS1 level. The former reflects MLCT, while the latter includes MLCT in part canceled by the transferred proton. The spin density on the Ru atom is 0.98 for $T_{MLCT\text{-}TA}$, further indicating one electron transfer from the metal to the pynp. The Ru spin density for $T_{MLCT\text{-}CA}$ is 0.82, indicating that the spin is delocalized in part from the metal to the OH ligand after ESPT (see SOMO1 of $T_{MLCT\text{-}CA}$ in Supporting Information Table S3). Quite different from the open question that persists in the homoleptic complexes[24] (such as [Ru(bpy)$_3$]) whether an electron is localized on a single ligand or delocalized over all of them in the emitting state MLCT state, there is no doubt that one electron in the MLCT state is transferred from Ru and is localized in single ligand pynp.

Concerning the triplet metal-centered states, there are two different minimum structures depending on the directions of σ^* (//H_2O and ⊥H_2O), termed as $T_{MC\text{-}CA}$ and $T_{MC\text{-}TA}$, as well as $T_{MC'\text{-}CA}$ and $T_{MC'\text{-}TA}$, respectively. As shown in Figure 2, one can see that the corresponding metal−ligand bonding is stretched and weakened substantially, as has been observed in the triplet metal-centered state of other similar Ru complexes.[24] In $T_{MC\text{-}CA}$, the Ru−water (O2) bond is stretched by about 0.4 Å, the Ru−N5 bond (*trans* to the Ru−water bond) is also elongated by about 0.3 Å, and the energy is increased by 29.2 kcal/mol, compared with $S_{0,CA}$. A similar elongation for the Ru−water and Ru−N3 (*trans* to O2) bond and destabilization by 22.6 kcal/mol are seen in $T_{MC\text{-}TA}$, relative to $S_{0,TA}$. In these T_{MC} structures, taking the Ru−O2 (water) as the *z* axis and the Ru−N6 as the *y* axis (Scheme 1), one electron is excited from the d_{xz} to the d_{z2} orbital which is σ^* (//H_2O) (Supporting Information Table S4) and thus the σ bonding in the *z* direction should become weaker. This nearly dissociative nature of water becomes important in the photoisomerization reaction mechanism, which is discussed in the following section. On the other hand, in the other MC structures called $T_{MC'}$ structures, the $d_{x2\text{-}y2}$ orbital is involved in the σ^*(⊥H_2O) orbital, and both Ru−N7 and Ru−N8 bonds are stretched by about 0.3 Å in the $T_{MC'\text{-}CA}$ and $T_{MC'\text{-}TA}$. In these structures, the Ru−water distance

dx.doi.org/10.1021/ct400982r | J. Chem. Theory Comput. 2014, 10, 668−675

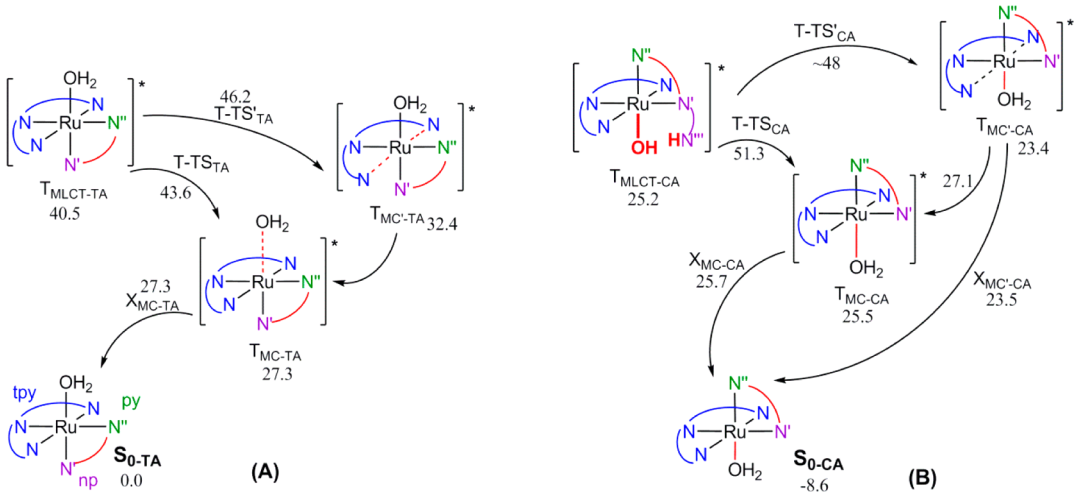

Figure 4. Schematic diagrams for the connection among S_0, T_{MLCT}, T_{MC}, and $T_{MC'}$ structures via approximate TSs in the regions of (A) *trans* and (B) *cis* isomers. Numbers shown for each structure are the relative energy (in kcal/mol).

is nearly unchanged and the water dissociation is not promoted. In all these T_{MC} structures, because of the local nature of the excitation, the dipole moment (Supporting Information Table S6) as well as the Ru atomic charge is changed little from the S_0 structures; the Ru spin density is nearly 2.

B. Photoisomerization Pathways. Potential energy surfaces (PESs) of photoisomerization between complexes TA and CA via both adiabatic and nonadiabatic pathways involving the singlet ground state and the lowest triplet state were investigated. The overall potential energy profile for the photoisomerization reaction is shown in Figure 3 (with relative energies summarized in Supporting Information Table S5).

Adiabatic Reaction Pathway on the Ground Singlet State S_0. The water dissociation process was proposed to occur as the initial step of the isomerization process.[5c−e] The present calculation shows that the Gibbs (electronic) energy cost for the water dissociation from $S_{0\text{-}TA}$ to give an intermediate $S_{0\text{-}TB}$ optimized without the H_2O ligand is 9.4 (21.3) kcal/mol. This is lower than that corresponding dissociation energy from $S_{0\text{-}CA}$ to give an intermediate $S_{0\text{-}CB}$, 13.7 (26.4) kcal/mol, due to a loss of H-bonding from CA. The detailed energetics of the water dissociation was further investigated by relaxed scan optimizations as a function of the Ru−O distance. The PESs for the water dissociation from $S_{0\text{-}TA}$ and $S_{0\text{-}CA}$ in S_0 increase continuously and monotonously. Also, full optimization starting from structures $S_{0\text{-}CB}$ or $S_{0\text{-}TB}$ with a water molecule placed at the Ru−O bond of ~5 Å directly leads to $S_{0\text{-}TA}$ or $S_{0\text{-}CA}$ without any barrier or intermediate, confirming that there is no transition state for the water dissociation.

The 5-coordniate intermediate $S_{0\text{-}CB}$ is a little more stable than $S_{0\text{-}TB}$, by 3.4 (3.5) kcal/mol, suggesting some repulsive interaction between the N4 lone pair and π electrons of the tpy ring in $S_{0\text{-}TB}$, as mentioned for $S_{0\text{-}CA}$ and $S_{0\text{-}TA}$ in the previous section. We found a transition state, TS($S_{0\text{-}TB}$-$S_{0\text{-}CB}$) (Figure 2), that connects two intermediates $S_{0\text{-}TB}$ and $S_{0\text{-}CB}$ with a barrier of about 13.8 (15.1) kcal/mol relative to $S_{0\text{-}TB}$ or 17.2 (18.6) kcal/mol relative to $S_{0\text{-}CB}$. At the TS, the pynp ligand has rotated within the N3−Ru−N5 plane and formed a Y-shape with the N6 atom of the tpy ligand, going from a T-shaped $S_{0\text{-}CB}$ through this TS to another T-shaped $S_{0\text{-}TB}$. We should note that the overall barrier of the thermal isomerization from $S_{0\text{-}TA}$ or $S_{0\text{-}CA}$ in the singlet state is quite high, ~23.2−30.9 (36.4−45.0) kcal/mol, and is also slightly higher in energy comparing with an isomerization TS in the triplet state (to be discussed below).

Adiabatic Reaction Pathway on the First Triplet State. Recently, the broadband femtosecond fluorescence-upconversion spectroscopy in the 440−690 nm range with a resolution of 110 ± 10 fs is used to capture the early relaxation processes leading to the triplet MLCT state of the prototype complex ($[Ru(bpy)_3]^{2+}$),[25] suggesting a decay time of 15 ± 10 fs, which is significantly shorter than the ultrafast decays[26] reported in previous transient-absorption[26a] and femtosecond fluorescence-upconversion experiments.[26f] Because of the similarity of the complex in the present study, the early relaxation process from S_{MLCT} to T_{MLCT} upon the irradiation is presumed to be highly efficient. Here, we did not address this relaxation process, mainly because of the uncertain reliability of the TD-DFT method and many closely lying states. As we discussed in the preceding section, we found two optimized metal−ligand charge-transfer minima, $T_{MLCT\text{-}TA}$ and $T_{MLCT\text{-}CA}$, corresponding to *trans* and *cis* isomers, respectively. Therefore, we investigated the isomerization pathways from these T_{MLCT} minima. The final overall potential energy profiles are shown in Figure 3. The details of the profiles in two dimensions will be discussed in the following paragraphs.

In the region of TA complexes, when appropriate initial MOs are used,[27] we were able to obtain the triplet MLCT and MC states simultaneously at certain geometries, and we use these states for the 1D relaxed scan with respect to R(Ru−OH_2), the distance between the Ru atom and the O atom in the OH_2, and the 2D rigid scan with respect to R(Ru−OH_2) and R(Ru−N3), the distance between Ru and N3, to determine the transition states connecting these states. In the following, we call the lowest point of crossing of the two states found in the scan as the "approximate TS", which is considered to be an excellent estimate of the real TS when two states couple very weakly as in this case.[28] A connection diagram thus obtained is shown in Figure 4A (Supporting Information Figure S2 for some details). In the pathway from $T_{MLCT\text{-}TA}$ to $T_{MC\text{-}TA}$ we found an approximate TS, T-TS_{TA}, at Ru−O = 2.344 Å and Ru−N3 = 2.15 Å with an electronic energy of 43.6 kcal/mol. An approximate TS, T-TS'_{TA}, was also found between $T_{MLCT\text{-}TA}$ to $T_{MC'\text{-}TA}$ lying at 46.2 kcal/mol by using a linearly interpolated scan,[24c] but the pathway connecting $T_{MC'\text{-}TA}$ to

dx.doi.org/10.1021/ct400982r | J. Chem. Theory Comput. 2014, 10, 668−675

$T_{MC\text{-}TA}$ was not studied in detail, as the direct path to $T_{MC\text{-}TA}$ through T-TS_{TA} is found to be more favorable.

As discussed in the preceding section about the region of the *cis* complex CA, in sharp contrast to $T_{MLCT\text{-}TA}$, ESPT has taken place in the *cis* triplet minimum of $T_{MLCT\text{-}CA}$. The relative energy of $T_{MLCT\text{-}CA}$ is 23.0 (25.2) kcal/mol, much lower than the *trans* counterpart $T_{MLCT\text{-}TA}$, 38.5 (40.5) kcal/mol. Two pathways from $T_{MLCT\text{-}CA}$, to $T_{MC\text{-}CA}$ and to $T_{MC'\text{-}CA}$, have been found also for the *cis* isomer (Figure 4B). The relaxed scan from the minimum structure of $T_{MLCT\text{-}CA}$ (with ESPT) showed that, as the Ru−O bond stretched, the reverse proton transfer from N4 to O2 occurred. In sharp contrast to a low barrier (in terms of electronic energy) of 3.1 kcal/mol for $T_{MLCT\text{-}TA}$ to T-TS_{TA}, the approximate adiabatic transition T-TS_{CA} from $T_{MLCT\text{-}CA}$ to $T_{MC\text{-}TA}$ is much higher in energy lying at ∼51.3 kcal/mol, with a high barrier of ∼26 kcal/mol from $T_{MLCT\text{-}CA}$. The approximate TS, T-TS_{CA}, from $T_{MLCT\text{-}CA}$ to $T_{MC'\text{-}CA}$ is at ∼42 kcal/mol, and $T_{MC'\text{-}CA}$ is connected to $T_{MC\text{-}CA}$ with an approximate TS of ∼27.1 kcal/mol. Different from the situation for TA, here the preferred pathway from $T_{MLCT\text{-}CA}$ is the one to the minimum of $T_{MC'\text{-}CA}$ which is unfortunately not the state related to the water dissociation.

Next, the behavior starting from the minimum of $T_{MC\text{-}TA}$ and $T_{MC\text{-}CA}$ along the water dissociation direction has been investigated by a relaxed scan. From $T_{MC\text{-}TA}$ or $T_{MC\text{-}CA}$ the PES increases slowly and continually without a transition state and reached the five-coordinate triplet state $T_{MC\text{-}TB}$ or $T_{MC\text{-}CB}$ without changing the nature of the metal-centered state. The electronic energy required for the water dissociation is 8.2 and 10.2 kcal/mol, respectively, which is in agreement with the experimental estimation (∼10.0 kcal/mol).[5c,d] Importantly, in the Gibbs energy, this process is slightly downhill without barrier (Figure 3) due to an entropic gain in this process. As shown in Figure 3, the five-coordinate $T_{MC\text{-}TB}$ and $T_{MC\text{-}CB}$ are found to isomerize very easily to each other via TS($T_{MC\text{-}TB}$-$T_{MC\text{-}CB}$) with a very small barrier, 0.2 (0.8) and 1.4 (0.6) kcal/mol from $T_{MC\text{-}TB}$ and $T_{MC\text{-}CB}$, respectively.

Overall, the adiabatic isomerization pathway from $T_{MLCT\text{-}TA}$ to $T_{MLCT\text{-}CA}$ involves five steps: conversion from $T_{MLCT\text{-}TA}$ to $T_{MC\text{-}TA}$ with a small barrier at T-TS_{TA}, water dissociation without barrier to give $T_{MC\text{-}TB}$, easy isomerization from $T_{MC\text{-}TB}$ to $T_{MC\text{-}CB}$, easy water recoordination to give $T_{MC\text{-}CA}$, and a high barrier from $T_{MC\text{-}CA}$ to $T_{MLCT\text{-}CA}$. The last step prevents the adiabatic conversion from $T_{MLCT\text{-}TA}$ to $T_{MLCT\text{-}CA}$ or vice versa.

Nonadiabatic Reaction Pathway via the First Triplet State. We further investigated the nonadiabatic pathways for photoisomerization by locating minimum energy crossing points (MSXs) between the first triplet state and the singlet ground state. As shown in Figure 3, six MSXs have been found (see Supporting Information Figures S4−S9 for details).

First, one recognizes that in the isomerization region the energy of the transition state on the triplet state TS($T_{MC\text{-}TB}$-$T_{MC\text{-}CB}$) at 21.7(36.3) kcal/mol is quite close to that of TS($S_{0\text{-}TB}$-$S_{0\text{-}CB}$) on the ground state at 23.2 (36.4) kcal/mol. Similar energies with similar structures suggest the existence of crossing points between the triplet/singlet PESs in the isomerization region. The minimum energy crossing $X_{MC\text{-}B}$ has actually been found between the MC-B ($T_{MC\text{-}TB}$ and $T_{MC\text{-}CB}$) triplet and the closed shell singlet state S_0 ($S_{0\text{-}TB}$ and $S_{0\text{-}CB}$) with the electronic energy of 35.1 kcal/mol. This provides a nonadiabatic pathway from the triplet to the ground state in the isomerization region.

Two MSXs, $X_{MC\text{-}TA}$ and $X_{MC\text{-}CA}$, were found very close both in geometry and energy to the hydrated MC excited complexes, $T_{MC\text{-}TA}$ and $T_{MC\text{-}CA}$, respectively, which also provide pathways to regenerate the ground-state reactant complexes, $S_{0\text{-}TA}$ and $S_{0\text{-}CA}$. Similarly, two MSXs, $X_{MC\text{-}TB}$ and $X_{MC\text{-}CB}$, were located very close to the dehydrated four-coordinate MC excited complexes, $T_{MC\text{-}TB}$ and $T_{MC\text{-}CB}$, respectively. The presence of these crossings provides channels to regenerate $S_{0\text{-}TB}$ and $S_{0\text{-}CB}$, which can recoordinate exothermically with a water molecule to give back the ground-state hydrated reactant complexes, $S_{0\text{-}TA}$ and $S_{0\text{-}CA}$. As shown in Figure 4, an MSX, $X_{MC'\text{-}CA}$, is also found to be near the minimum of $T_{MC'\text{-}CA}$, which also regenerates the ground-state reactant complex $S_{0\text{-}CA}$ but is not related to the isomerization pathway.

Mechanistic Picture of the Irreversible Photoisomerization. The main mechanism of the irreversible photoisomerization of the present Ru(II) aqua complex, investigated by the present systematic DFT study, can be summarized as follows, as roughly illustrated in Scheme 2. Upon the UV−visible light

Scheme 2. Schematic Diagram of the Major Working Mechanism for the Irreversible Photoisomerization Pathway[a]

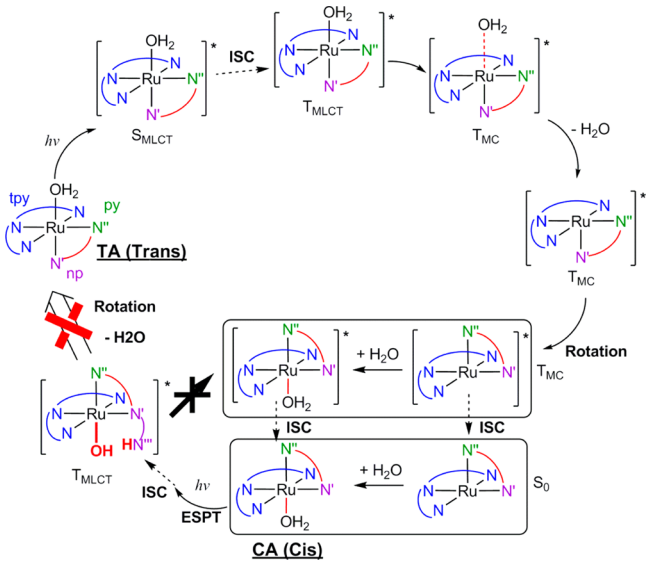

[a]Non-productive decays are not shown.

irradiation, the reactant complex is excited mainly to a singlet metal−ligand charge transfer (S_{MLCT}) state of the complex, which can undergoes ultrafast relaxation to a thermally equilibrated T_{MLCT} state. For TA, starting from the minimum of the $T_{MLCT\text{-}TA}$ state, there is a small barrier of only 3.1 kcal/mol to overcome T-TS_{TA} and then reach to $T_{MC\text{-}TA}$, on which the water dissociation occurs without a Gibbs energy barrier, to reach $T_{MC\text{-}TB}$. With the absence of water, the pynp ligand of the intermediate $T_{MC\text{-}TB}$ can easily rotate along an N−Ru−N axis to afford the intermediate $T_{MC\text{-}CB}$ with a very small barrier of ∼0.2 (0.8) kcal/mol. Following the forward direction on the adiabatic pathway, one water recoordinates from the other side of the tpy plane to reach the minimum of the $T_{MC\text{-}CA}$ state. Due to the much higher barrier to overcome T-TS_{CA}, the existence of the crossing point $X_{MC\text{-}CA}$ provides the decay channel to $S_{0\text{-}CA}$. In addition, the existence of another crossing point, $X_{MC\text{-}CB}$, supplies a decay channel to the ground state $S_{0\text{-}CB}$, followed by one water recoordination also to form $S_{0\text{-}CA}$. Thus

dx.doi.org/10.1021/ct400982r | J. Chem. Theory Comput. 2014, 10, 668−675

nonadiabatic pathways are the dominant pathways for photochemical isomerization from TA to CA. On the other hand, photoisomerixation from CA to TA is prohibited by the existence of the highly stabilized $T_{MLCT\text{-}CA}$, in which excited-state proton transfer has taken place and a strong Ru(II)−OH bond is formed. The CA complex cannot get past this minimum because of high barriers around it and is eventually relaxed back to $S_{0\text{-}CA}$. The dissipation of energy here is supposed to take place by ultrafast intramolecular vibrational-energy redistribution (IVR) transferring the energy stored in the high-frequency modes to the low-frequency modes, which is believed in the prototype complex[25] and observed in the case of bacteriorhodopsin.[29]

CONCLUSION

The working mechanism uncovered by the present DFT study solves the puzzle of why photoisomerization in the Ru(II) complexes is irreversible. The dissociative nature of the T_{MC} state leads to the easy water removal and then the five-coordinate intermediates can isomerize via rotation of the pynp ligand. However, upon the irradiation, the complexes have been mainly populated to the singlet MLCT (with the largest oscillator strength), which then undergo ultrafast decay to triplet MLCT. During this process, the excited-state proton transfer (ESPT) takes place only in CA and forms a very strong Ru(II)−OH bond. Therefore, the isomerization from the *cis* isomer to the *trans* isomer is suppressed. Moreover, such a high reaction barrier also prevents the isomerization process from TA to CA solely on the adiabatic triplet pathway. Instead, crossing points ($X_{MC\text{-}CB}$, $X_{MC\text{-}CA}$) near the minimum of the triplet metal-centered state for the *cis* isomer provide (nonadiabatic) decay channels to $S_{0\text{-}CA}$ and, thus, complete the photoisomerization pathway from TA to CA. The dynamic effects that control the concurrent pathways at the early stage are under our further investigation.

ASSOCIATED CONTENT

Supporting Information

Figures S1−S9, Tables S1−S8, and Cartesian coordinates of the optimized structures. This material is available free of charge via the Internet at http://pubs.acs.org.

AUTHOR INFORMATION

Corresponding Author

*E-mail: keiji.morokuma@emory.edu.

Notes

The authors declare no competing financial interest.

ACKNOWLEDGMENTS

L.D. thanks Dr. Satoshi Maeda very much for helpful assistance on the GRRM program. This work is supported in part by Japan Science and Technology Agency (JST) with a Core Research for Evolutional Science and Technology (CREST) grant in the Area of High Performance Computing for Multiscale and Multiphysics Phenomena and Grants-in-Aid for Scientific Research <KAKENHI> Nos. 24245005 and 25109525 from Japan Society for the Promotion of Science (K.M.). The computational resources at Research Center of Computer Science (RCCS) of the Institute for Molecular Science (IMS) and at ACCMS of Kyoto University are acknowledged.

REFERENCES

(1) (a) Allen, M. T.; Whitten, D. G. *Chem. Rev.* **1989**, *89*, 1691−1702. (b) Waldeck, D. H. *Chem. Rev.* **1991**, *91*, 415−436. (c) Tamai, N.; Miyasaka, H. *Chem. Rev.* **2000**, *100*, 1875−1890. (d) Natansohn, A.; Rochon, P. *Chem. Rev.* **2002**, *102*, 4139−4176. (e) Liu, F.; Morokuma, K. *J. Am. Chem. Soc.* **2012**, *134*, 4864−4876. (f) Tzeli, D.; Theodorakopoulos, G.; Petsalakis, I. D.; Ajami, D.; Rebek, J. *J. Am. Chem. Soc.* **2012**, *134*, 4346−4354.

(2) (a) Sekharan, S.; Katayama, K.; Kandori, H.; Morokuma, K. *J. Am. Chem. Soc.* **2012**, *134*, 10706−10712. (b) Ryazantsev, M. N.; Altun, A.; Morokuma, K. *J. Am. Chem. Soc.* **2012**, *134*, 5520−5523. (c) Li, X.; Chung, L. W.; Morokuma, K. *J. Chem. Theory Comput.* **2011**, *7*, 2694−2698.

(3) (a) Ando, R.; Mizuno, H.; Miyawaki, A. *Science* **2004**, *306*, 1370−1373. (b) Li, X.; Chung, L. W.; Mizuno, H.; Miyawaki, A.; Morokuma, K. *J. Phys. Chem. Lett.* **2010**, *1*, 3328−3333. (c) Li, X.; Chung, L. W.; Mizuno, H.; Miyawaki, A.; Morokuma, K. *J. Phys. Chem. B* **2010**, *114*, 1114−1126.

(4) McClure, B. A.; Mockus, N. V.; Butcher, D. P.; Lutterman, D. A.; Turro, C.; Petersen, J. L.; Rack, J. J. *Inorg. Chem.* **2009**, *48*, 8084−8091.

(5) (a) Durham, B.; Wilson, S. R.; Hodgson, D. J.; Meyer, T. J. *J. Am. Chem. Soc.* **1980**, *102*, 600−607. (b) Planas, N.; Vigara, L.; Cady, C.; Miró, P.; Huang, P.; Hammarström, L.; Styring, S.; Leidel, N.; Dau, H.; Haumann, M.; Gagliardi, L.; Cramer, C. J.; Llobet, A. *Inorg. Chem.* **2011**, *50*, 11134−11142. (c) Yamazaki, H.; Hakamata, T.; Komi, M.; Yagi, M. *J. Am. Chem. Soc.* **2011**, *133*, 8846−8849. (d) Boyer, J. L.; Polyansky, D. E.; Szalda, D. J.; Zong, R.; Thummel, R. P.; Fujita, E. *Angew. Chem., Int. Ed.* **2011**, *50*, 12600−12604. (e) Padhi, S. K.; Fukuda, R.; Ehara, M.; Tanaka, K. *Inorg. Chem.* **2012**, *51*, 5386−5392. (f) Kayanuma, M.; Gindensperger, E.; Daniel, C. *Dalton Trans.* **2012**, *41*, 13191−13203. (g) Gindensperger, E.; Koppel, H.; Daniel, C. *Chem. Commun.* **2010**, *46*, 8225−8227. (h) Heydová, R.; Gindensperger, E.; Romano, R.; Sykora, J.; Vlcek, A., Jr.; Zális, S.; Daniel, C. *J. Phys. Chem. A* **2012**, *116*, 11319−11329. (i) El Nahhas, A.; van der Veen, R. M.; Penfold, T. J.; Pham, V. T.; Lima, F. A.; Abela, R.; Blanco-Rodriguez, A. M.; Zális, S.; Vlcek, A.; Tavernelli, I.; Rothlisberger, U.; Milne, C. J.; Chergui, M. *J. Phys. Chem. A* **2013**, *117*, 361−369.

(6) (a) Ishizuka, T.; Tobita, K.; Yano, Y.; Shiota, Y.; Yoshizawa, K.; Fukuzumi, S.; Kojima, T. *J. Am. Chem. Soc.* **2011**, *133*, 18570−18573. (b) Miyazaki, S.; Kojima, T.; Fukuzumi, S. *J. Am. Chem. Soc.* **2008**, *130*, 1556−1557.

(7) (a) Concepcion, J. J.; Jurss, J. W.; Templeton, J. L.; Meyer, T. J. *J. Am. Chem. Soc.* **2008**, *130*, 16462−16463. (b) Yagi, M.; Tajima, S.; Komi, M.; Yamazaki, H. *Dalton Trans.* **2011**, *40*, 3802−3804. (c) Wasylenko, D. J.; Ganesamoorthy, C.; Koivisto, B. D.; Henderson, M. A.; Berlinguette, C. P. *Inorg. Chem.* **2010**, *49*, 2202−2209. (d) Masaoka, S.; Sakai, K. *Chem. Lett.* **2009**, *38*, 182−183. (e) Concepcion, J. J.; Jurss, J. W.; Norris, M. R.; Chen, Z.; Templeton, J. L.; Meyer, T. J. *Inorg. Chem.* **2010**, *49*, 1277−1279. (f) Concepcion, J. J.; Tsai, M.-K.; Muckerman, J. T.; Meyer, T. J. *J. Am. Chem. Soc.* **2010**, *132*, 1545−1557.

(8) (a) Alezra, V.; Bernardinelli, G.; Corminboeuf, C.; Frey, U.; Kundig, E. P.; Merbach, A. E.; Saudan, C. M.; Viton, F.; Weber, J. *J. Am. Chem. Soc.* **2004**, *126*, 4843−4853. (b) Rapaport, I.; Helm, L.; Merbach, A. E.; Bernhard, P.; Ludi, A. *Inorg. Chem.* **1988**, *27*, 873−879. (c) Stebler-Roethlisberger, M.; Hummel, W.; Pittet, P. A.; Buergi, H. B.; Ludi, A.; Merbach, A. E. *Inorg. Chem.* **1988**, *27*, 1358−1363.

(9) Vlcek, A., Jr.; Zalis, S. *Coord. Chem. Rev.* **2007**, *251*, 258−287.

(10) (a) Daniel, C. *Coord. Chem. Rev.* **2003**, *238*−*239*, 143−166. (b) Bossert, J.; Daniel, C. *Coord. Chem. Rev.* **2008**, *252*, 2493−2503. (c) Kayanuma, M.; Daniel, C.; Koppel, H.; Gindensperger, E. *Coord. Chem. Rev.* **2011**, *255*, 2693−2703. (d) Escudero, D.; Gonzalez, L. *J. Chem. Theory. Comput.* **2012**, *8*, 203−213.

(11) (a) Salassa, L.; Garino, C.; Salassa, G.; Gobetto, R.; Nervi, C. *J. Am. Chem. Soc.* **2008**, *130*, 9590−9597. (b) Göttle, A. J.; Dixon, I. M.; Alary, F.; Heully, J.-L.; Boggio-Pasqua, M. *J. Am. Chem. Soc.* **2011**, *133*,

9172−9174. (c) Lutterman, D. A.; Rachford, A. A.; Rack, J. J.; Turro, C. *J. Phys. Chem. A* **2009**, *113*, 11002−11006.
(12) Zhao, Y.; Truhlar, D. *Theor. Chem. Acc.* **2008**, *120*, 215−241.
(13) Escudero, D.; Gonzalez, L. *J. Chem. Theory. Comput.* **2012**, *8*, 203−213.
(14) Zhao, Y.; Truhlar, D. G. *Acc. Chem. Res.* **2008**, *41*, 157−167.
(15) Hay, P. J.; Wadt, W. R. *J. Chem. Phys.* **1985**, *82*, 270−283.
(16) McLean, A. D.; Chandler, G. S. *J. Chem. Phys.* **1980**, *72*, 5639−5648.
(17) Frisch, M. J.; Trucks, G. W.; Schlegel, H. B.; Scuseria, G. E.; Robb, M. A.; Cheeseman, J. R.; Scalmani, G.; Barone, V.; Mennucci, B.; Petersson, G. A.; Nakatsuji, H.; Caricato, M.; Li, X.; Hratchian, H. P.; Izmaylov, A. F.; Bloino, J.; Zheng, G.; Sonnenberg, J. L.; Hada, M.; Ehara, M.; Toyota, K.; Fukuda, R.; Hasegawa, J.; Ishida, M.; Nakajima, T.; Honda, Y.; Kitao, O.; Nakai, H.; Vreven, T.; Montgomery, J. A., Jr.; Peralta, J. E.; Ogliaro, F.; Bearpark, M.; Heyd, J. J.; Brothers, E.; Kudin, K. N.; Staroverov, V. N.; Kobayashi, R.; Normand, J.; Raghavachari, K.; Rendell, A.; Burant, J. C.; Iyengar, S. S.; Tomasi, J.; Cossi, M.; Rega, N.; Millam, J. M.; Klene, M.; Knox, J. E.; Cross, J. B.; Bakken, V.; Adamo, C.; Jaramillo, J.; Gomperts, R.; Stratmann, R. E.; Yazyev, O.; Austin, A. J.; Cammi, R.; Pomelli, C.; Ochterski, J. W.; Martin, R. L.; Morokuma, K.; Zakrzewski, V. G.; Voth, G. A.; Salvador, P.; Dannenberg, J. J.; Dapprich, S.; Daniels, A. D.; Farkas, Ö.; Foresman, J. B.; Ortiz, J. V.; Cioslowski, J.; Fox, D. J. *Gaussian 09*, revision A.2.; Gaussian, Inc.: Wallingford, CT, 2009.
(18) (a) Maeda, S.; Ohno, K.; Morokuma, K. *J. Chem. Theory Comput.* **2010**, *6*, 1538−1545. (b) Maeda, S.; Ohno, K.; Morokuma, K. *Phys. Chem. Chem. Phys.* **2013**, *15*, 3683−3701.
(19) Maeda, S.; Osada, Y.; Morokuma, K.; Ohno, K. GRRM11, see http://grrm.chem.tohoku.ac.jp/SRPS/GRRMe.HTM (accessed November 20, 2012).
(20) (a) Cossi, M.; Rega, N.; Scalmani, G.; Barone, V. *J. Comput. Chem.* **2003**, *24*, 669−681. (b) Cossi, M.; Barone, V. *J. Chem. Phys.* **2001**, *115*, 4708−4717. (c) Barone, V.; Cossi, M. *J. Phys. Chem. A* **1998**, *102*, 1995−2001.
(21) Marenich, A. V.; Cramer, C. J.; Truhlar, D. G. *J. Phys. Chem. B* **2009**, *113*, 6378−6396.
(22) (a) Rillema, D. P.; Jones, D. S.; Woods, C.; Levy, H. A. *Inorg. Chem.* **1992**, *31*, 2935−2938. (b) Stoyanov, S. R.; Villegas, J. M.; Rillema, D. P. *Inorg. Chem.* **2002**, *41*, 2941−2945.
(23) A reviewer suggested a possible ESPT involving a solvent water molecule that may form a hydrogen bond with N4 or N3 of the np ligand. However, the Ru center is coordinatively saturated and cannot work as the OH^- acceptor after proton transfer.
(24) (a) Heully, J.-L.; Alary, F.; Boggio-Pasqua, M. *J. Chem. Phys.* **2009**, *131*, 184308. (b) Alary, F.; Heully, J.-L.; Bijeire, L.; Vicendo, P. *Inorg. Chem.* **2007**, *46*, 3154−3165. (c) Alary, F.; Boggio-Pasqua, M.; Heully, J.-L.; Marsden, C. J.; Vicendo, P. *Inorg. Chem.* **2008**, *47*, 5259−5266.
(25) Cannizzo, A.; van Mourik, F.; Cawelda, W.; Zgrablic, G.; Bressler, C.; Chergui, M. *Angew. Chem., Int. Ed.* **2006**, *45*, 3174−3176.
(26) (a) Damrauer, N. H.; Cerullo, G.; Yeh, A.; Boussie, T. R.; Shank, C. V.; McCusker, J. K. *Science* **1997**, *275*, 54−57. (b) Damrauer, N. H.; McCusker, J. K. *J. Phys. Chem. A* **1999**, *103*, 8440−8446. (c) McCusker, J. K. *Acc. Chem. Res.* **2003**, *36*, 876−887. (d) McClure, B. A.; Abrams, E. R.; Rack, J. J. *J. Am. Chem. Soc.* **2010**, *132*, 5428−5436. (e) Rachford, A. A.; Rack, J. J. *J. Am. Chem. Soc.* **2006**, *128*, 14318−14324. (f) Bhasikuttan, A. C.; Suzuki, M.; Nakashima, S.; Okada, T. *J. Am. Chem. Soc.* **2002**, *104*, 8398−8405.
(27) When a T_{MLCT} state is obtained in the triplet DFT calculation in the region away from a crossing point, on the other side of the crossing a T_{MC} state is usually obtained in the triplet DFT calculation. In the vicinity of the crossing, two distinct states can be obtained for the same geometry. If MOs for the T_{MLCT} state above are used as the initial guess, the T_{MLCT} state will be obtained; if MOs for the T_{MC} state above are used as the initial guess, the T_{MC} state will be obtained. Of course, sometimes only one state may converge with the other state diverged or converged to the same state.
(28) In general two diabatic states cross with each other. Our two triplet states (MLCT and MC states) are not quite diabatic and form a TS via weak coupling. People often call this "crossing", but it is actually a TS on an adiabatic PES. We did not fully optimized this TS but call the structure where two scanned PESs became equal as the "approximate TS", which should be a very good estimate of the real TS when two states couple very weakly, as in the present case.
(29) Kobayashi, T.; Saito, T.; Ohtani, H. *Nature* **2001**, *414*, 531−534.